

Article

Discovery of First-in-Class, Potent and Orally Bioavailable EED inhibitor with Robust Anti-cancer Efficacy

Ying Huang, Jeff Zhang, Zhengtian Yu, Hailong Zhang, Youzhen Wang, Andreas Lingel, Wei Qi, X. Justin Gu, Kehao Zhao, Michael David Shultz, Long Wang, Xingnian Fu, Yongfeng Sun, Qiong Zhang, Xiangqing Jiang, Jiang-wei Zhang, Chunye Zhang, Ling Li, Jue Zeng, Lijian Feng, Chao Zhang, Yueqin Liu, Man Zhang, Lijun Zhang, Mengxi Zhao, Zhenting Gao, Xianghui Liu, Douglas Fang, Haibing Guo, Yuan Mi, Tobias Gabriel, Michael P Dillon, Peter Atadja, and Counde Oyang

J. Med. Chem., **Just Accepted Manuscript** • DOI: 10.1021/acs.jmedchem.6b01576 • Publication Date (Web): 16 Jan 2017

Downloaded from <http://pubs.acs.org> on January 16, 2017

Just Accepted

“Just Accepted” manuscripts have been peer-reviewed and accepted for publication. They are posted online prior to technical editing, formatting for publication and author proofing. The American Chemical Society provides “Just Accepted” as a free service to the research community to expedite the dissemination of scientific material as soon as possible after acceptance. “Just Accepted” manuscripts appear in full in PDF format accompanied by an HTML abstract. “Just Accepted” manuscripts have been fully peer reviewed, but should not be considered the official version of record. They are accessible to all readers and citable by the Digital Object Identifier (DOI®). “Just Accepted” is an optional service offered to authors. Therefore, the “Just Accepted” Web site may not include all articles that will be published in the journal. After a manuscript is technically edited and formatted, it will be removed from the “Just Accepted” Web site and published as an ASAP article. Note that technical editing may introduce minor changes to the manuscript text and/or graphics which could affect content, and all legal disclaimers and ethical guidelines that apply to the journal pertain. ACS cannot be held responsible for errors or consequences arising from the use of information contained in these “Just Accepted” manuscripts.

1
2
3
4
5
6
7
8
9
10
11
12
13
14
15
16
17
18
19
20
21
22
23
24
25
26
27
28
29
30
31
32
33
34
35
36
37
38
39
40
41
42
43
44
45
46
47
48
49
50
51
52
53
54
55
56
57
58
59
60

	Dillon, Michael; Ideaya Biosciences , Atadja, Peter; Novartis Institutes for Biomedical research, Biology Oyang, Counde; China Novartis Institutes for BioMedical Research Co., Ltd.

SCHOLARONE™
Manuscripts

TITLE

Discovery of First-in-Class, Potent and Orally Bioavailable EED inhibitor with Robust Anti-cancer Efficacy

Ying Huang^{*†}, Jeff Zhang[†], Zhengtian Yu[†], Hailong Zhang^{†‡}, Youzhen Wang^{†§}, Andreas Lingel[‡], Wei Qi[†], Justin Gu[†], Kehao Zhao^{†§}, Michael D. Shultz^{†§}, Long Wang[†], Xingnian Fu[†], Yongfeng Sun[†], Qiong Zhang[†], Xiangqing Jiang[†], Jiangwei Zhang[†], Chunye Zhang[†], Ling Li[†], Jue Zeng[†], Lijian Feng[†], Chao Zhang^{†¶}, Yueqin Liu[†], Man Zhang^{†¶}, Lijun Zhang[†], Mengxi Zhao[†], Zhenting Gao[†], Xianghui Liu^{†¶}, Douglas Fang[†], Haibing Guo^{†¶}, Yuan Mi[†], Tobias Gabriel^{†¶}, Michael P. Dillon^{‡¶}, Peter Atadja[†], Counde Oyang[†]

[†]Novartis Institutes for BioMedical Research, 4218 Jinke Road, Shanghai 201203, China

[‡]Novartis Institutes for BioMedical Research, 5300 Chiron Way, Emeryville, California 94608, United States

*Corresponding author:

Ying Huang

Address: 4218 Jinke Road, Zhangjiang Hi-Tech Park, Pudong New Area, Shanghai 201203, China

Tel: 86-18621082695

Keywords:

Epigenetic, allosteric inhibition, fragment-based drug discovery, PRC2, oncology, EED

ABSTRACT

Overexpression and somatic heterozygous mutations of EZH2, the catalytic subunit of Polycomb repressive complex 2 (PRC2), are associated with several tumor types. EZH2 inhibitor, EPZ-6438 (Tazemetostat), demonstrated clinical efficacy in patients with acceptable safety profile as monotherapy. EED, another subunit of PRC2 complex, is essential for its histone methyltransferase activity through direct binding to trimethylated lysine 27 on histone 3 (H3K27Me3). Herein we disclose the discovery of a first-in-class potent, selective and orally bioavailable EED inhibitor compound **43** (EED226). Guided by X-ray crystallography, compound **43** was discovered by fragmentation and regrowth of Compound **7**, a PRC2 HTS hit that directly binds EED. The ensuing scaffold hopping followed by multi-parameter optimization led to the discovery of **43**. Compound **43** induces robust and sustained tumor regression in EZH2^{MUT} pre-clinical DLBCL model. For the first time we demonstrate that specific and direct inhibition of EED can be effective as an anti-cancer strategy.

■ INTRODUCTION

Tumorigenesis is believed to involve multiple epigenetic alterations, in addition to genetic aberrations, that contribute to the progressive transformation of normal cells towards a malignant phenotype. As a result, novel cancer therapies that work by reversing epigenetic effects are being increasingly explored.¹ Post-translational modifications of core histone proteins of chromatin are one of the major epigenetic mechanisms regulating gene expression, and paramount among them are methylation events at lysine and arginine residues, catalyzed by histone methyltransferases (HMTs).²

Polycomb repressive complex 2 (PRC2) is a multiprotein complex that catalyzes the methylation of histone H3 at lysine 27 (H3K27). Trimethylated H3K27 (H3K27Me3) is a repressive post-translational modification.³ Overexpression, gain-of-function mutations of EZH2 and hypertrimethylation of H3K27 have been implicated in a myriad of cancers.⁴ The polycomb group (PcG) proteins SUZ12, EED, EZH2 (or its homolog EZH1), RBBP4, and RBBP7 constitute the “core PRC2”; removal of core subunits by genetic or RNAi-based approaches destabilizes EZH2 and results in the abrogation of all PRC2 functions.⁵ More importantly, it was known that the recognition of H3K27Me3 by WD40-repeats containing β -propeller protein EED is essential in stimulating basal PRC2 activity and propagating H3K27 methylation in repressive chromatin for gene silencing.⁶ EED selectively binds the positively charged quaternary amine of the trimethylated lysine via a so-called “aromatic cage” formed by Phe97, Tyr148 and Tyr365, while the neighboring Trp364 interacts with the aliphatic sidechain of the lysine residue.^{6a} EZH2 or EZH1 acts as the catalytic subunit of PRC2.⁷ Despite high sequence identity, EZH2 and EZH1 are not functionally redundant and have different expression patterns. While EZH2 is found only in actively dividing cells, EZH1 is found in both dividing and non-dividing cells.

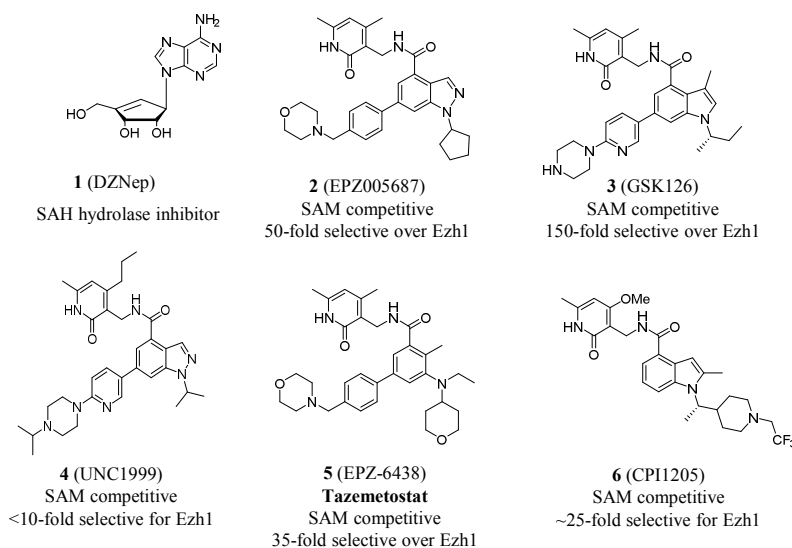


Figure 1: Selected PRC2 inhibitors

Although PRC2 containing EZH1 (PRC2–EZH1) has lower catalytic activity compared to that containing EZH2 (PRC2–EZH2), both complexes contribute to the maintenance of cellular H3K27 methylation states.

Given the association of PRC2/EZH2 with cancer, multiple biotech and pharmaceutical companies have been actively pursuing compounds that can effectively inhibit PRC2 activity (Figure 1). The first such compound was 3-deazaneplanocin A (**1**, DZNep) which interferes with S-adenosyl-L-homocysteine (SAH).⁸ Although the compound has very short plasma half-life, significant antitumor activity in various cancer types was reported, along with toxicities possibly due to nonspecific inhibition of histone methylation. This result further spurred interest in development of specific PRC2 inhibitors. In 2012, Epizyme and GSK reported the development of S-adenosylmethionine (SAM)-competitive inhibitors **2** (EPZ005687)⁹ and **3** (GSK-126),¹⁰ respectively, resulting from optimization of hits identified from high-throughput screenings. Compound **3** markedly inhibits the growth of lymphomas carrying activating EZH2 mutations *in vivo*. Following this, compound **4** (UNC1999) was reported as the first orally bioavailable EZH2

inhibitor that was highly selective for both wild-type and Y641 mutant EZH2, and as well as EZH1.¹¹ Shortly after, compound **5** (EPZ-6438) was reported as Epizyme's second generation EZH2 inhibitor with better potency and good oral bioavailability.¹² Based on the encouraging efficacies in preclinical studies, phase 1/2 clinical trials of compound **5** in advanced solid tumors and B cell lymphomas was launched in June 2013. In the meantime, compound **3** and compound **6** (CPI-1205)¹³ from Constellation also entered clinical trials in EZH2-mutant B cell NHL and SMARCB1-deficient tumors, respectively. With three independent EZH2 inhibitors in clinical trials, a trove of data is expected on both potential toxicity and efficacy of this approach. However, all three PRC2 inhibitors currently in clinic (compound **5**: NCT01897571, NCT02601937, NCT02601950; compound **3**: NCT02082977; compound **6**: NCT02395601) are pyridone-derived SAM-competitive inhibitors targeting EZH2 with relative weaker activity against EZH1.

It has been reported that binding of H3K27Me3 to EED allosterically activates the methyltransferase activity of PRC2.^{6a} This could partially be explained by the recently published high resolution crystal structures of PRC2 complex, which suggested that this interaction induces conformational change of stimulation-responsive motif (SRM) in EZH2, leading to enhanced catalytic efficiency.¹⁴ We hypothesized that low molecular weight (LMW) compounds interacting with PRC2 via the "Me3 pocket" of EED may inhibit the methyltransferase activities of both PRC2-EZH2 and PRC2-EZH1, and therefore may provide therapeutic(s) similar or complementary to the EZH2 inhibitors in clinic.

▪ RESULTS and DISCUSSION

In order to find LMW compounds that antagonize PRC2 complex activity, we initiated a high-throughput screening (HTS) campaign, which used the recombinant 5-member PRC2 complex as

enzyme, H3[21-44, K27Me0] as a peptide substrate, and homogeneous time resolved fluorescence (HTRF) method to detect the dimethylated product. The mechanisms of action of the screening hits were further elucidated by various competition studies using SAM, H3K27Me0 substrate peptide, and/or K27Me3 stimulation peptide. Compound 7 (Figure 2a) was identified as a K27Me3-competitive inhibitor in biochemical assays, and its binding to EED through K27Me3 pocket via the “aromatic cage” was further confirmed by X-ray crystallography (PDB accession code: 5H19, details of the hits finding are reported in a separate manuscript).^{15,18}

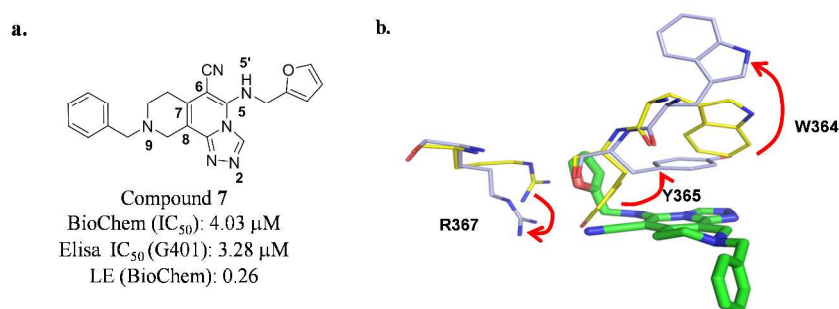


Figure 2: (a) Chemical structure of HTS hit compound 7. (b) More significant movement of key residues upon binding of compound 7 compared to binding of K27Me3 (green: compound 7, PDB accession code: 5H19; blue: EED residues binding to compound 7; yellow: EED residues binding to K27Me3; K27Me3 peptide is not showed for the purpose of clarity; movement of the residues are indicated by red arrows).

Although the dynamic nature of the Me3 pocket, especially the flexibility of the side-chains of Trp364 and Arg367, has been previously reported by comparing the K27Me3 bound structure to apo EED protein structure,^{6c} binding of compound 7 induced more substantial conformational change of side-chains of Trp364 and Tyr365, in addition to Arg367 (Figure 2b). As a result, a much deeper pocket was induced with the calculated druggability score improved from previously reported 0.64¹⁶ to 0.96. Encouraged by this finding, we started our discovery efforts to optimize compound 7 in order to discover potential LMW therapeutic agents targeting the K27Me3 pocket of EED.

During the SAR investigation, biological activities of our compounds were assessed in a cascade of assays (Supporting Information). To determine the binding affinity of the compounds to EED, we developed an EED-H3K27me3 peptide alphascreen binding assay and performed competition studies with our compounds. At the same time, the biochemical inhibitory activities of the compounds were evaluated with a liquid chromatography mass spectrometry (LC-MS) based assay which detects SAH formation using either H3K27Me0 peptide or nucleosome as substrate.¹⁷ Since results from the two assays correlate reasonably well, in this publication the SAR is discussed only with biochemical activities although alphascreen assay was routinely ran as part of SAR support.¹⁸ Furthermore, the ability of compounds to reduce global K27Me3 at cellular level was assessed in G401 cells with an ELISA assay. Anti-proliferative activity of selected compounds was determined in KARPAS-422 cells, a diffuse large B-cell lymphoma (DLBCL) cell line harboring a monoallelic Y641N EZH2 mutation. Since we also observed the reported slow kinetics of the antiproliferative activity for SAM-competitive EZH2 inhibitors,^{10, 12b} IC₅₀'s at 14 day were required to differentiate *in vitro* anti-tumor activity for the compounds. Compound 7, with IC₅₀ of 0.62 μ M in alphascreen binding assay, IC₅₀ of 4.03 μ M in biochemical assay with H3K27Me0 peptide as substrate, and ELISA IC₅₀ of 3.28 μ M in G401 cells, represented an excellent starting point for us to start our optimization efforts.

Fragmentation and regrowth: bicyclic triazolopyridine as scaffold I

The key interactions in the binding of compound 7 include two hydrogen bonds and a set of π - π interactions. The two hydrogen bonds, one between hydrogen on 5'-amino and the side chain carbonyl of Asn194 (red dash, Figure 3a), and another one between nitrogen at 2-position with side-chain of Lys211, appear to offer key polar interactions. The π - π interactions, taking full advantage of the aromatic cage residues, also play indispensable roles. Firstly, the electron-

deficient bicyclic [1,2,4]triazolo[4,3-a]pyridine core is held in place by π - π stacking interactions with the electron-rich Tyr148 and Tyr365. Secondly, the electron-rich furan forms a π - π stacking interaction with guanidinium group of Arg367, and an edge-to-face interaction with Tyr365, which we referred to as “deep pocket” interactions, since the furan group is located in the inner part of the induced pocket. Additionally, the CN group at C6 seems interaction with multiple

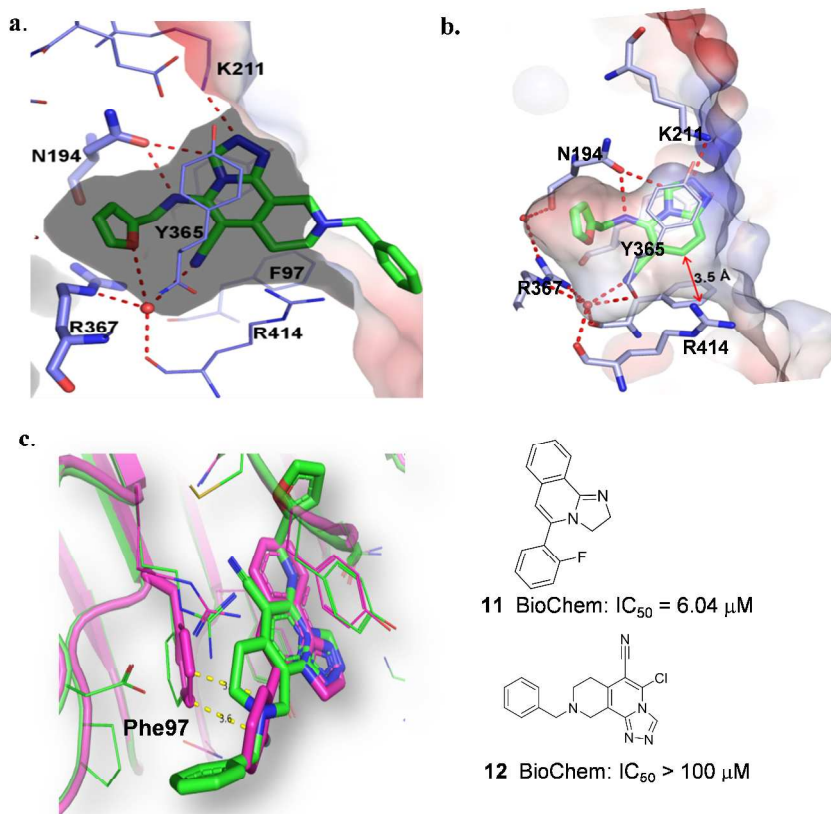


Figure 3: Structural basis for fragmentation and regrowth: (a) Key interactions of compound 7 with EED (PDB accession code: 5H19) (b) Compound 8 bound to EED (PDB accession code: 5H24) (c) Overlay of compound 7 and 11 bound to EED (PDB accession code: 5H25) (green: compound 7; magenta: compound 11)

residues through a water network. (Figure 3a, see Supporting Information (Figure S1) for details of the interactions). Upon closer inspection of the interactions between compound 7 and EED, it appeared to us that the entire piperidine ring connecting C7 to C8 and the benzyl group attached

to nitrogen at 9-position did not contribute much to the interaction, and likely reduced efficiency of binding due to the non-essential lipophilicity. Compound **8**, a fragment of compound **7** (Table 1), which was confirmed to retain most of the key interactions with EED (Figure 3b), is equipotent as compound **7**. This transformation led to dramatic improvements of both ligand efficiency (LE) and lipophilic efficiency (LipE) (Table 1).

With what appeared to be the minimal pharmacophore required for binding, we set out to improve potency for **8**. The co-crystal structure of compound **8** with EED suggested C8 to be a more attractive vector for additional substitution as compared to C7 (red arrow, Figure 3b).

Meanwhile, the surprising activities of compound **11** (Figure 3c), another HTS hit, caught our attention. The two key features critical to the binding to EED, the electron-rich “deep pocket” aryl group and hydrogen bond donating NH at 5'-position, are missing in compound **11**; and the importance of “the deep pocket” was attested by total loss of activities in compound **12** (Figure 3c). We postulate that an edge-to-face interaction between the phenyl ring of compound **11** and Phe97 (Figure 3c) possibly contributed most to its activity in the absence of “the deep pocket” group. Furthermore, when the co-crystal structure of compound **11** was overlaid with that of compound **7**, we hypothesized that the aryl substitution at 8-position of compound **8** would mimic that of compound **11** and help us pick up this edge-to-face interaction. Compound **9** (Table 1) was therefore designed and synthesized, and a close to 20-fold improvement in biochemical activity was achieved, with slight decrease in LE and LipE. Substitutions at C8 position are mostly solvent exposed and achieving additional interactions with the protein was challenging, however some interesting SAR were observed. Addition of a (dimethylamino)methyl group at 4'-position of C8 aryl group (compound **10**), improved

biochemical potency 7-fold, and this effect was also observed with similar amino tails and at both 4'- and 3'-position of the C8 aryl group (unpublished results).

Compounds in table 1 were synthesized according to the reaction sequence depicted in Scheme 1. 2-Cyanoacetamide was condensed with ethyl propiolate under basic condition to afford dihydroxylated pyridine compound **14**, which was brominated to afford compound **15**.

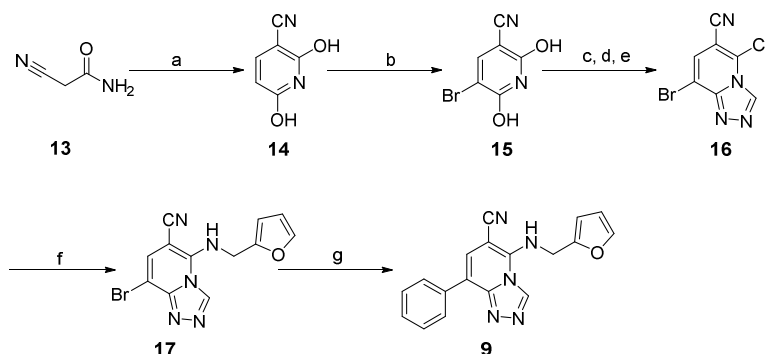
Table 1: Discovery of bicyclic 6-CN triazolopyridine lead compound **9**: fragmentation of hit compound **7** and regrowth

compound	Structure	BioChem (IC ₅₀ , μM) ^a	clogP ^b	LE (BioChem) ^c	LipE (BioChem) ^d
7		4.03	2.87	0.26	2.6
8		1.00	0.98	0.46	5.0
9		0.062	2.87	0.42	4.4
10		0.009	2.70	0.40	5.3

^aIC₅₀ values reported as an average ≥ 2 determinations; see Supporting Information for further details; ^bclogP values generated via ChemBioDraw version 14.0.0.117; ^cLE = ligand efficiency = pIC₅₀ – HAC; ^dLipE = lipophilic efficiency = pIC₅₀ – cLogP.

compound **15** was treated with POCl₃, followed by aqueous hydrazine solution and then cyclized to give the desired bicyclic 8-bromo-[1,2,4]triazolo[4,3-a]pyridine derivative **16**. Displacement with furan-2-ylmethanamine at room temperature in ethanol afforded compound **17**, which was converted to desired target compound **9** after Suzuki coupling with phenylboronic acid.

Scheme 1: Synthesis of 5-((furan-2-ylmethyl)amino)-8-phenyl-[1,2,4]triazolo[4,3-a]pyridine-6-carbonitrile



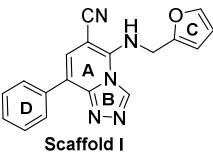
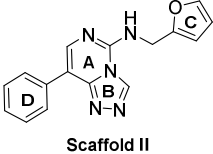
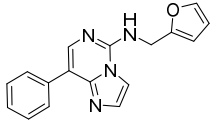
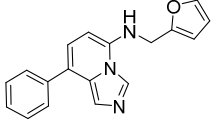
Reagents and conditions: (a) NaOMe, ethyl propiolate, 90°C, 2h, 79%; (b) Br₂, acetic acid, 63%; (c) POCl₃, 160°C, 2h, 27%; (d) NH₂NH₂, 0°C, 93%; (e) CH(OMe)₃, TFA, 0°C, 67%; (f) furan-2-ylmethanamine, EtOH, rt, 73%; (g) phenylboronic acid, PdCl₂(dppf), NaHCO₃, dioxane-H₂O, 90 °C overnight, 10%.

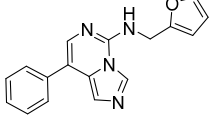
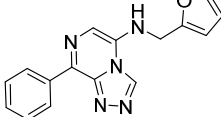
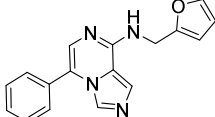
Core permutation: [1,2,4]triazolo[4,3-c]pyrimidine core as scaffold II

To continue our SAR exploration, we carried out systematic scaffold hopping efforts of the [6, 5] bicyclic core (Table 2). Removal of the cyano group at the 6-position of compound **9** and replacing it with nitrogen led to compound **18** with similar potency and slightly improved LE and LipE, which is possibly due to a newly formed water-mediated hydrogen bond network (supporting information, Figure S1). Having the nitrogen atom at 6-position seems to be critical to the binding. Shifting the nitrogen to 7-position as in compound **22** decreased activity over 60-fold vs. compound **18**, and removing this nitrogen resulted in a potency decrease over 50-fold (compound **21** vs. compound **20**). The accessibility of nitrogen at the 2-position as a hydrogen bond acceptor to Lys211 also plays a pivotal role in binding; removing this nitrogen resulted in a 400-fold drop in potency (compound **19** vs. compound **18**). Although the nitrogen at 1-position does not seem to contribute to meaningful polar interaction judging from X-ray structures,

removing the nitrogen led to a 5-fold drop in potency from compound **18** to **21**, which is possibly due to less effective π - π interactions with a less electron-deficient bicyclic core. In addition to pyrimidine-based bicyclic core, we also investigated their pyrazine-based counterparts, such as compounds **22** and **23**. In all the cases we examined, alteration of the heterocyclic core of **18** was detrimental to potency. Nonetheless, we had two very promising scaffolds in our hand, namely, 8-aryl-[1,2,4]triazolo[4,3-a]pyridine (Scaffold I) and 8-aryl-[1,2,4]triazolo[4,3-c]pyrimidine (Scaffold II) for further optimization, and we were intrigued to determine if the SAR at the C-ring and D-ring were transferable between the two scaffolds.

Table 2: Discovery of bicyclic 6-CN triazolopyridine lead compound **9**: fragmentation of hit compound **7** and regrowth

compound	Structure	BioChem (IC ₅₀ , μ M) ^a	clogP ^b	LE (BioChem) ^c	LipE (BioChem) ^d
9	 Scaffold I	0.062	2.87	0.41	4.3
18	 Scaffold II	0.052	2.78	0.45	4.5
19		20.49	3.54	0.21	1.2
20		14.80	4.18	0.22	0.55

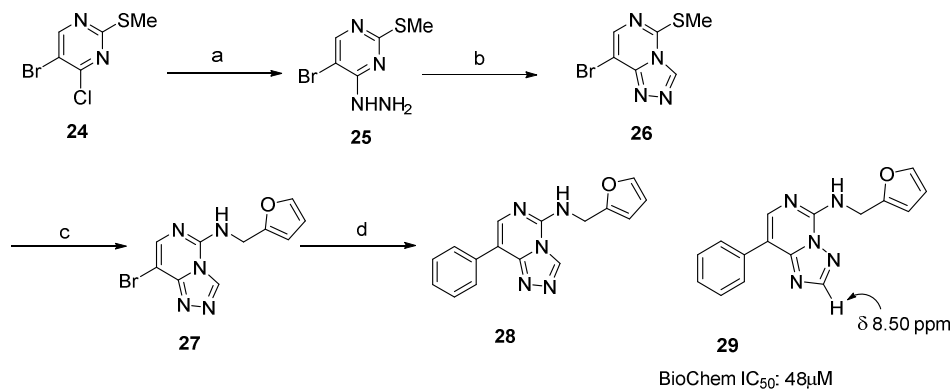
21		0.26	3.54	0.30	3.0
22		3.52	2.99	0.25	2.5
23		2.18	3.75	0.26	1.91

^aIC₅₀ values reported as an average ≥ 2 determinations; see Supporting Information for further details; ^bclogP values generated via ChemBioDraw version 14.0.0.117; ^cLE = ligand efficiency = pIC₅₀ – HAC; ^dLipE = lipophilic efficiency = pIC₅₀ – cLogP.

Synthesis of the analogs for 8-aryl-[1,2,4]triazolo[4,3-c]pyrimidine (Scaffold II) is detailed in Scheme 2. Commercially available 5-bromo-4-chloro-2-(methylthio)pyrimidine (compound **24**) was treated with hydrazine, followed by trimethyl orthoformate to afford bicyclic compound **26**, which was transformed to compound **27** after selective displacement with furan-2-ylmethanamine at the 5-position. Compound **27** was further converted to the 8-phenyl analog **28** after Suzuki reaction. In some cases when stronger bases were used, Dimroth rearrangement¹⁹ product **29** was also observed. By using NaHCO₃, we were able to prepare compound **28** in multi-gram scales with minimum formation of side product **29**. Compound **29** can be separated, and its identity was distinctive from singlet at δ 8.50 in ¹H NMR accounting for the proton at C2. When profiled in our biochemical assay, compound **29** lost most of the activity of its isomer **28**, which is consistent with the notion that the H-bond acceptor to Lys211 at the 1-position of the bicyclic system is important to maintain the interaction with EED.

Syntheses of the compounds in Table 2 with bicyclic cores other than [1,2,4]triazolo[4,3-a]pyridine-6-carbonitrile and [1,2,4]triazolo[4,3-c]pyrimidine are reported in the supporting information.

Scheme 2. N-(furan-2-ylmethyl)-8-phenyl-[1,2,4]triazolo[4,3-c]pyrimidin-5-amine



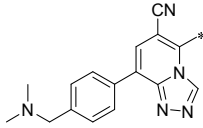
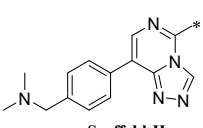
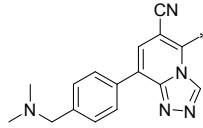
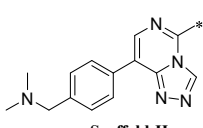
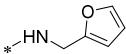
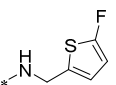
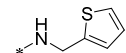
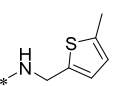
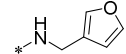
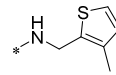
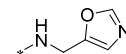
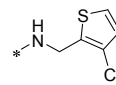
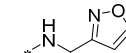
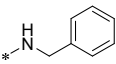
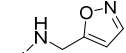
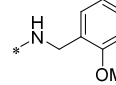
Reagents and conditions: (a) hydrazine, rt, 4h, 92%; (b) CH(OMe)₃, reflux, 3h, 92%; (c) furan-2-ylmethanamine, rt, 16.7%; (d) phenylboronic acid, PdCl₂(dppf), NaHCO₃, dioxane-H₂O, 90°C overnight, 10%.

SAR investigation of “the deep pocket”

Next, we turned our attention to the deep pocket or C-ring SAR for both scaffold I and II, in search for a replacement for the potentially metabolically labile furan ring.²⁰ Electron-rich 5-membered rings, such as furan, are preferred, regardless of the position of the oxygen as seen in compounds **10a** & **10b** vs. **31a** & **31b** (Table 3). Thiophene isosteres are generally tolerated, albeit slightly less potent than their furan counterparts as in compound **30a** & **30b**. Compounds bearing less electron-rich C-rings, such as oxazole, isoxazole and thiazole, are generally less potent. Overall, SAR of the C-ring is quite similar in both scaffolds until substitutions were introduced onto the ring. In both scaffolds, small substitution at the 5'-position of C ring, such as F (**39a** & **b**) is more tolerated than the larger substitutions (**40a** & **b**). The two scaffolds started to behave quite differently when substitutions were introduced at 3'-position; the

substitutions were tolerated in Scaffold II, but not tolerated in Scaffold I, when comparing **37b** vs **37a**, and **38b** vs **38a**. The same differences were also observed in 6-membered ring, as in compound **39a-40a** vs **39a-40b**. We believe in Scaffold I there is a steric clash between the CN and the 3'-substituted on the C ring that resulted in the subtle difference in SAR between

Table 3: Investigation of SAR in “the deep pocket” (C-ring)

<div>  <p>Scaffold I</p> </div> <div>  <p>Scaffold II</p> </div> <div>  <p>Scaffold I</p> </div> <div>  <p>Scaffold II</p> </div>									
R ₁	Cmpd	BioChem (IC ₅₀ , μM) ^a	Cmpd	BioChem (IC ₅₀ , μM) ^a	R ₁	Cmpd	BioChem (IC ₅₀ , μM) ^a	Cmpd	BioChem (IC ₅₀ , μM) ^a
	10a	0.013	10b	0.013		35a	0.51	35b	0.15
	30a	0.020	30b	0.093		36a	2.22	36b	12.4
	31a	0.009	31b	0.019		37a	21.8	37b	0.049
	32a	0.15	32b	0.29		38a	2.34	38b	0.053
	33a	0.069	33b	0.77		39a	21.8	39b	0.049
	34a	0.069	34b	0.13		40a	14.9	40b	0.094

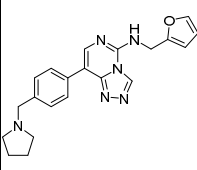
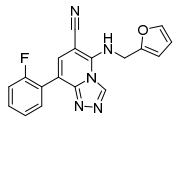
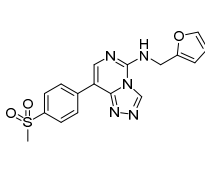
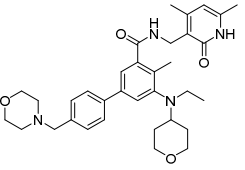
^aIC₅₀ values reported as an average ≥2 determinations; see Supporting Information for further details.

scaffold I and II. At this point, we concluded this particular quest without finding a viable replacement for furan in the deep pocket.

Selection of compound for pharmacology studies

We next turned our attention to optimization of the D-ring. For reasons unclear to us, the gain of potency in biochemical assay from varying solvent-exposed D-ring mostly diminished in the 14-day anti-proliferative activities in KARPAS-422 (Table 4). We therefore relied on overall

Table 4. Selection of *in vivo* candidate based on compound potency and pharmacokinetic profile

Compound		41	42	43	5
structures					
BioChem	IC ₅₀ (μM) ^a	0.007	0.030	0.022	0.002
	LE ^b	0.37	0.41	0.37	0.28
	LipE ^c	4.4	4.5	6.4	5.3
G401Elisa (IC ₅₀ , μM) ^d		0.032	0.21	0.22	0.040
KARPAS 14D IC ₅₀ (μM) ^e		0.088	0.076	0.080	0.012
MLM (hER) ^f		0.52	0.80	0.36	0.77
f _u (% free) ^g		38.1	2.81	14.4	1.4
dnAUC-iv (nM*hr) ^h		765	1751	534	1303
dnAUC-po (nM*hr)	Whole ⁱ	531	714	5648	254
	Free ^j	202	20.1	813	4
Cl (ml/min/kg) ^k		57	29	8	22
Vdss (L/kg) ^l		1.9	0.7	0.8	1.2
T _{1/2} (hr) ^m		0.6	0.4	2.2	1.6
F% (po) ⁿ		71	42	109	20

^aIC₅₀ values reported as an average of more than determinations see Supporting Information for further details; ^bLE = ligand efficiency = pIC₅₀ – HAC; ^cLipE = lipophilic efficiency = pIC₅₀ – cLogP; ^dGlobal H3K27me3 levels measured in G401 cells and IC₅₀ values reported as an average of more than two determinations; ^eIC₅₀ value reported for compound **41** and **42** as single determination, while that of compounds **43** reported as an average of 10 measurements with SD = 0.019 and that of **5** as an average of 2 measurement with SD = 0.006 ; ^fHepatic extraction ratio of compounds in mouse liver microsomes; ^gFraction unbound to plasma protein (expressed in % unbound); ^hDose-normalized total exposure following intravenous (iv) dosing of 1 mg/kg in male CD-1 mice, formulated in PEG300:Soltuol HS15:pH4.65 acetate buffer (20:10:70, v/v/v); ⁱDose-normalized total exposure following per os

(po) dosing of 2 mg/kg in male CD-1 mice, formulated in PEG300:Solutol HS15:pH4.65 acetate buffer (20:10:70, v/v/v); ¹Dose-normalized free AUC following po dosing; ²Cl = plasma clearance; ³V_{dss} = volume of distribution at steady state; ⁴t_{1/2} = terminal half-life; ⁵Oral bioavailability.

pharmacokinetic profiles to select our compound that would enable head-to-head comparison with the reported EZH2 inhibitor(s) in mouse efficacy studies.

Compounds were evaluated in mouse liver microsome (MLM) assays and also in male CD-1 mice for *in vivo* PK properties at dosed at 1 mg/kg intravenous (iv) and 2 mg/kg orally (po).

Overall, hepatic extraction rates in MLM predicted fairly well the *in vivo* total clearance of the compounds, suggestive of hepatic clearance being the major clearance pathway. Among the three EED compounds shown in Table 4, compound **43** (*N*-(furan-2-ylmethyl)-8-(4-(methylsulfonyl)phenyl)-[1,2,4]triazolo[4,3-*c*]pyrimidin-5-amine) stood out as having very low *in vivo* and *in vitro* clearance, and approximately 100% oral bioavailability. Compound **43** has low volume of distribution (0.8 L/kg), reasonable terminal t_{1/2} (2.2 h), and moderate plasma protein binding (PPB), approximately 10-fold greater free fraction than that of compound **5** at 14.4% & 1.5%, respectively. Together this led to free normalized AUC free in CD-1 mice at 813 nM*hr in comparison to that at 4 nM*hr for compound compound **5**. This 200-fold higher free-exposure of compound **43** counters well against the 8-fold lower anti-proliferation activity in the 14-day assay than compound **5**. In CD-1 mouse, compound **43** achieved sufficient targets coverage for at least 8 hours (Supporting Information, Figure S2) at 2 mg/kg. Taken together, the data suggest that compound **43** constitutes a reasonable candidate for pharmacology studies.

Efficacy studies

Compound **43** was then profiled at high doses in mouse pharmacokinetic studies. In the subsequent tolerability test in CD-1 mice, dosing of compound **43** for 14 days at 300 mg/kg bid was well tolerated with no apparent adverse effects (Supporting Information, Figure S39(a)). Further pharmacology studies were carried out in the KARPAS-422 derived DLBCL model in

Balb/C nude mice. Complete tumor regression (10/10 CR) was observed with treatment of compound **43** at 300 mg/kg bid for 34 days (Figure 4). After treatment of compound **43** was stopped, no tumor regrowth was observed in 4 out of the 5 animals kept for observation during the entire 5 months. With the single regrowth that was observed at approximately 130 days, spontaneous regression occurred (Figure 4).

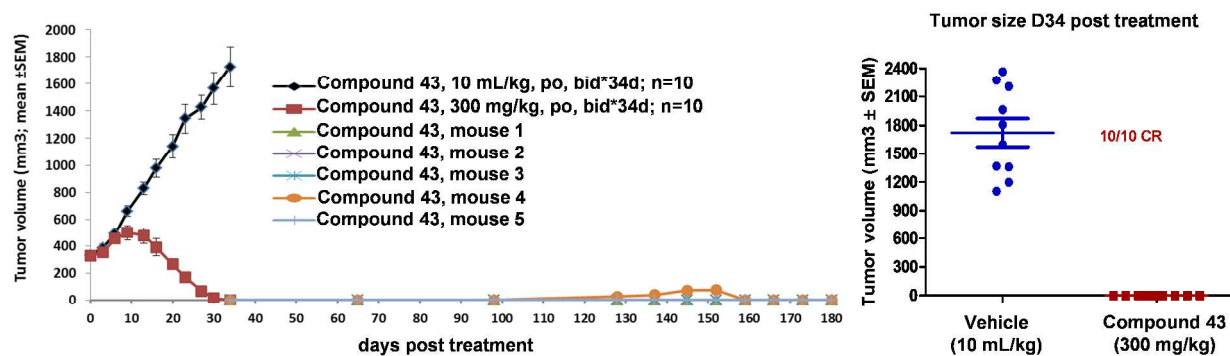


Figure 4. Pharmacology studies of compound **43** in KARPAS-422 derived DLBCL model in Balb/C nude mice at 300 mg/kg (bid, suspension, n =10)

We next performed dose de-escalation studies to determine the minimal efficacious dose and to establish dose dependent efficacy (Supporting Information, Figure S3(b)). After two weeks of treatment, differentiated growth patterns started to emerge between the lower dose groups (1.5 & 4 mg/kg) and higher dose group (12 & 40 mg/kg). Global H3K27Me3 levels in tumors was used as our pharmacodynamics markers, which decreased dose-dependently along with the target genes upregulation after 21 days of compound dosing, and all showing good correlation with the plasma exposure of compound **43**.¹⁸

Compound **43** is a highly selective EED inhibitor with drug-like properties

To confirm the on-target binding of compound **43** to the H3K27Me3 pocket, we obtained high resolution crystal structures of EED (76-441) in complex with compound **43** and EZH2 (40-68) peptide (EBD) (PDB accession code: 5GSA). Compound **43** retained all the interactions of its parent compound **7** (*supra vide*) with EED, while in addition the phenyl ring of the mostly

solvent exposed *p*-methanesulfonylphenyl group picks up edge-to-face π - π interaction with side-chain of Phe97. Compound **43** was subsequently profiled in our in-house histone methyltransferase panel including close to 30 HMT targets. Compound **43** is highly selective against all other targets (>10,000 fold) except EZH1, with almost identical potency as EZH2. In our safety pharmacology panel including 59 targets,²¹ compound **43** shown <50% inhibition at the highest concentration tested (10 μ M or 30 μ M). IC₅₀'s in hERG binding assay and QPatch assay are both well above 30 μ M.

Table 4. Characterization of compound **43**

MW	MP (°C)	clogP ^a	Caco-2 (A>B, 10 ⁻⁶ cm/s / ratio)	Solubility				
				HT- Sol (mM) ^b	with crystalline material (mg/mL)			
					pH7	pH3	SGF ^c	Fassif ^d
369.4	207.6	1.22	3.0 / 7.6	0.012	0.025	0.026	0.055	0.035

In vitro ADME		In vivo PK	Mouse	Rat	Dog
In vitro LM (hER%, M/R/D/CM/H) ^e	36/14/41/27/25	dnAUC(nM*h) (p.o.) ^h	5648	1871	1907
In vitro hepatocytes (hER%, M/R/D/CM/H) ^f	25/22/51/30/20	Cl (mL/min/kg) ⁱ	8	14	16
f _u (M/R/D/H) ^g	15/8/24/13	F (%) ^j	109	60	68

^aclogP values generated via ChemBioDraw version 14.0.0.117; ^bEquilibrium solubility; ^csimulated gastric fluid; ^dfasted state simulated intestinal fluid; ^eHepatic extraction ratio of compound in mouse (M), rat (R), dog (D), cyno-monkey (CM) and human (H) liver microsomes; ^fHepatic extraction ratio of compound in mouse (M), rat (R), dog (D), cyno-monkey (CM) and human (H) hepatocytes; ^gUnbound fraction of compound to mouse (M), rat (R), dog (d) and human (h) plasma protein; ^hDose-normalized free AUC after po dosing, 2 mg/kg in male Sprague Dawley rat and 2 mg/kg in male Beagle dog, formulated with PEG300:Solutol HS15:pH4.65 acetate buffer (10:10:80, v/v/v); ⁱCl = total clearance; ^jOral bioavailability.

Compound **43** was further evaluated for its physicochemical properties and other DMPK parameters (Table 4). The solubility was relatively low, and with little dependency on the pH of the medium. Compound **43** has moderate permeability as the measured in Caco-2 cells at A→B

= 3.0×10^{-6} cm/s, with an efflux ratio at 7.6. When iv/oral PK studies were performed in rat and dogs (Table 5), we found that the *in vivo* clearances measured were well predicted by *in vitro* incubation experiments with liver microsome and hepatocytes. Given low *in vitro* clearance across all preclinical species, and the high predictive value of *in vitro* hepatocytes assays for compound **43**, clearance in human was projected to be low (< 5 mL/min/kg, ER <25%). The promising pharmacokinetic profile of compound **43** in all animal species tested, together with the results from its *in vitro* safety profile and superb efficacy in the xenograft model, support compound **43** for further evaluation.

▪ CONCLUSIONS

Herein, we report discovery of compound **43**, a first-in-class EED inhibitor. Compound **43** is a highly potent, efficient and selective inhibitor of EZH2 and EZH1 evaluated against a broad range of epigenetic and non-epigenetic targets. This inhibitor potently reduced global H3K27Me3 mark in cells and demonstrated selectively cell killing effects in cells carrying a heterozygous Y641N mutation. With favorable pharmacokinetic properties, compound **43** demonstrated very impressive anti-tumor activities in mouse xenograft model. For the first time we have demonstrated that inhibiting methyltransferase activity of PRC2 through binding to the K27Me3 pocket of EED could constitute a viable strategy for developing anti-cancer therapeutics. Together with extensive preclinical profiling results of compound **43**, especially its favorable pharmacokinetic profile and tolerability in preclinical animal species, compound of this type may be suitable for assessing long-term effects of pharmacologically inhibiting both EZH2 and EZH1 in preclinical models, and potentially in clinic, in terms of therapeutic benefits and potential toxicity.

▪ EXPERIMENTAL SECTION

Synthesis and Characterization: Unless otherwise mentioned, all reagents and solvents were obtained from commercial sources and used without purification. In some cases, intermediates were characterized by LC-MS to confirm that the mass matched the structure and carried on to the next step without further purification. Air sensitive procedures were performed under an atmosphere of nitrogen or argon. Purification of the final compounds to > 95% purity was carried out either using prepacked silica gel cartridge (Analogix, Biotage or ISCO) or reverse phase C18 column. ¹H (300 MHz) and ¹³C (100 MHz) NMR spectra were recorded on a Bruker AC300 spectrometer. NMR chemical shift (δ) are quoted in parts per million (ppm) referenced to the residual solvent peak [DMSO-d₆] set at 2.49 ppm or [CDCl₃] set at 7.26 ppm. Purity of all compounds was determined to be >95% by analytical HPLC.

5-((Furan-2-ylmethyl)amino)-8-phenyl-[1,2,4]triazolo[4,3-a]pyridine-6-carbonitrile (9): 8-Bromo-5-((furan-2-ylmethyl)amino)-[1,2,4]triazolo[4,3-a]pyridine-6-carbonitrile (compound 17) (40 mg, 0.13 mmol), phenylboronic acid (18.40 mg, 0.15 mmol), PdCl₂(dppf) (4.60 mg, 6.3 μmol) and NaHCO₃ (31.7 mg, 0.38 mmol) in dioxane (2 mL) and H₂O (1 mL) was heated to at 90°C under N₂ overnight. The resulting mixture was cool to room temperature, and H₂O was added to the mixture and extracted with EtOAc. The combined organic layers were dried (Na₂SO₄), filtered and concentrated. The residue was purified by basic prep-HPLC to afford 3.8 mg (10%) of the title compound. ¹H-NMR (400 MHz, DMSO-d₆) δ ppm 9.45 (s, 1 H), 8.87 (t, 1 H), 8.12 (d, *J* = 1.2 Hz, 1 H), 8.11 (s, 1 H), 7.68 (d, *J* = 0.8 Hz, 1 H), 7.66 (s, 1 H), 7.38 - 7.48 (m, 3 H), 6.46 - 6.54 (m, 2 H), 5.03 - 5.05 (d, *J* = 6 Hz, 2 H). LC-MS (*m/z*): 315.9 [M+H]⁺

2,6-Dihydroxynicotinonitrile (14): To a suspension of 2-cyanoacetamide (250 g, 2.55 mol) in methanol (1000 mL) was added NaOMe (137.8 g, 2.55 mol) at 0°C under N₂. The reaction mixture was stirred at the same temperature for 30 min. Ethyl propiolate (214.4 g, 2.55 mol) was

added dropwise at 0°C. The reaction mixture was stirred at 0°C for 2 h, then at 90°C for 2 h. The reaction mixture was then cooled to rt, and the resulting yellow paste was filtered. The filter cake was suspended with water and neutralized with concentrated HCl till pH reached ~6. A mixed solvent of DCM-MeOH (v/v = 20/1) was added and stirred at 0°C for 30 min. The solid was filtered and washed with Et₂O to give 274 g (79 %) of the title compound as yellow solid. ¹H-NMR (400 MHz, DMSO-d₆) δ ppm 9.88 (s, 1 H), 7.16 (d, *J* = 9 Hz, 1 H), 5.06 (d, *J* = 9 Hz, 1 H). LC-MS (m/z): 137.1 [M+H]⁺

5-Bromo-2,6-dihydroxynicotinonitrile (15): A suspension of 2,6-dihydroxynicotinonitrile (274 g, 2 mol) in acetic acid (1500 mL) was stirred at 70 °C for 30 min. To the mixture at 10°C was added a solution of Br₂ (100 mL, 2 mol) in acetic acid (100 mL). The resulting mixture was stirred for 20 min. The solid was filtered to give 271 g (63%) of the title compound as light yellow solid. ¹H-NMR (400 MHz, DMSO-d₆) δ ppm 7.86 (s, 1 H). LC-MS (m/z): 212.9 [M+H]⁺

8-Bromo-5-chloro-[1,2,4]triazolo[4,3-a]pyridine-6-carbonitrile (16): A solution of compound **15** (130 g, 0.6 mol) in POCl₃ (500 mL) was sealed and heated at 160°C for 2 h. The mixture was cooled to room temperature and concentrated to remove extra POCl₃. Ethyl acetate (2000 mL) and ice-water (2000 mL) was added to the residue and the resulting mixture was neutralized with aqueous NaHCO₃ until pH reached ~7. The aqueous layer was separated and extracted with ethyl acetate. The combined organic layers were washed with brine, dried (Na₂SO₄), filtered and concentrated. The mixture was purified with silica gel column chromatograph (eluted with PE-EA: 50/1) to give 41 g (27%) of the 5-bromo-2, 6-dichloronicotinonitrile compound as light yellow solid. ¹H-NMR (400 MHz, DMSO-d₆) δ ppm 9.10 (s, 1 H). LC-MS (m/z): 250.5 [M+H]⁺

8-Bromo-5-((furan-2-ylmethyl)amino)-[1,2,4]triazolo[4,3-a]pyridine-6-carbonitrile (17): To a mixture of compound **16** (1.03 g, 4 mmol) in EtOH (7 mL) at room temperature was added

1
2
3 furan-2-ylmethanamine (0.855 g, 8.80 mmol) in EtOH (1 mL) dropwise. The resulting mixture
4
5 was stirred at room temperature for 2 h under N₂. After the starting material was consumed,
6
7 DCM (20 mL) was added. Solvent was removed under vacuum after silica gel (~4 g) was added.
8
9 The silica gel coated with crude product was loaded on a silica gel column and eluted with
10
11 DCM-MeOH to give 1.2 g (94%) of the title compound as a light green solid. ¹H-NMR
12
13 (400MHz, DMSO-d₆) δ ppm 9.63 (s, 1 H), 8.85 (s, 1 H), 7.73 (s, 1 H), 7.66 (d, *J* = 0.8 Hz, 1 H),
14
15 6.51 (d, *J* = 2.8 Hz, 1 H), 6.44 (dd, *J* = 3.2, 2 Hz, 1 H), 4.97 (s, 2 H). LC-MS (m/z): 318.0.
16
17
18
19 [M+H]⁺
20
21
22

23 **5-Bromo-4-hydrazinyl-2-(methylthio)pyrimidine (25):** To a solution of 5-bromo-4-chloro-2-
24
25 (methylthio)pyrimidine (**24**, 49.0 g, 0.205 mol) in ethanol (1000 mL) was added hydrazine (21.5
26
27 g, 0.43 mol). The reaction was stirred at room temperature for 4 h. The resulting suspension was
28
29 filtered, washed with hexane and dried *in vacuo* to give the title compound (44.1 g, 92%) as a
30
31 white solid. ¹H-NMR (400 MHz, DMSO-d₆) δ ppm 8.08 (s, 1H), 2.42 (s, 3H). LC-MS (m/z):
32
33 234.9, 236.9 [M+H]⁺
34
35
36

37 **8-Bromo-5-(methylthio)-[1,2,4]triazolo[4,3-c]pyrimidine (26):** Compound **25** (40.0 g, 0.17
38
39 mol) was dissolved in 200 mL triethoxymethane. The mixture was heated at reflux and stirred for
40
41 3 h. The reaction mixture was concentrated under reduced pressure, and the residue was purified
42
43 by flash chromatography (eluted with EA: PE = 1:15~1:1) to give the title compound (38.3 g,
44
45 92%) as a white solid. ¹H-NMR (400 MHz, methanol-d₄) δ ppm 8.87 (s, 1H), 8.03 (s, 1H), 2.82
46
47 (s, 3H). LC-MS (m/z): 245.0, 247.0 [M+H]⁺
48
49
50
51

52 **8-Bromo-N-(furan-2-ylmethyl)-[1,2,4]triazolo[4,3-c]pyrimidin-5-amine (27):** 8-Bromo-5-
53
54 (methylthio)-[1,2,4]triazolo[4,3-c]pyrimidine (**26**) (100 mg, 0.408 mmol) was dissolved in furan-
55
56 2-ylmethanamine (1.5 mL). The mixture was stirred at rt for 1 h. The solvent was removed and
57
58
59
60

the residue was purified with silica gel column chromatography, eluted with DCM-MeOH (20:1), to give 20 mg (16.7%) of the title compound. $^1\text{H-NMR}$ (400 MHz, CD_3OD) δ ppm 9.28 (s, 1H), 7.87 (s, 1H), 7.47 (s, 1H), 6.38 - 6.40 (m, 2H), 4.77 (s, 2H). LC-MS (m/z): 294.0, 296.0 $[\text{M}+\text{H}]^+$

***N*-(Furan-2-ylmethyl)-8-phenyl-[1,2,4]triazolo[4,3-*c*]pyrimidin-5-amine (28):** To a solution of 8-bromo-*N*-(furan-2-ylmethyl)-[1,2,4]triazolo[4,3-*c*]pyrimidin-5-amine (20.0 mg, 0.068 mmol) in mixed solvent (dioxane: MeCN: water = 3 mL: 0.3 mL: 0.3 mL) was added potassium carbonate (28.2 mg, 0.204 mmol), phenylboronic acid (8.3 mg, 0.068 mmol) and $\text{Pd}(\text{PPh}_3)_4$ (7.86 mg, 6.80 μmol). The resulting mixture was stirred in microwave under N_2 at 110°C for 20 min. The mixture was then cooled to room temperature and solvent was removed *in vacuo*. The residue was purified with silica gel chromatography (eluted with DCM-MeOH (10:1)) to give 5 mg (22.3%) of the title compound **28**: $^1\text{H-NMR}$ (400 MHz, Methanol- d_4) δ 9.30 (s, 1H), 7.94 – 7.88 (m, 3H), 7.52 – 7.44 (m, 3H), 7.39 (t, $J = 7.4$ Hz, 1H), 6.44 (d, $J = 3.0$ Hz, 1H), 6.41 – 6.38 (m, 1H), 4.84 (s, 2H). LC-MS (m/z): 292.1 $[\text{M}+\text{H}]^+$ **29**: $^1\text{H-NMR}$ (400 MHz, Methanol- d_4) δ 8.30 (s, 1H), 8.04 (s, 1H), 7.81 – 7.72 (m, 2H), 7.40 – 7.32 (m, 3H), 7.30 – 7.23 (m, 1H), 6.26 (d, $J = 1.7$ Hz, 2H), 4.74 (s, 2H). LC-MS (m/z): 292.1 $[\text{M}+\text{H}]^+$

***N*-(Furan-2-ylmethyl)-8-(4-(methylsulfonyl)phenyl)-[1,2,4]triazolo[4,3-*c*]pyrimidin-5-amine (43):** To a solution of 8-bromo-*N*-(furan-2-ylmethyl)-[1,2,4]triazolo[4,3-*c*]pyrimidin-5-amine (20.0 mg, 0.068 mmol) in mixed solvent (dioxane: MeCN: water = 3 mL: 0.3 mL: 0.3 mL) was added potassium carbonate (28.2 mg, 0.204 mmol), (4-(methylsulfonyl)phenyl)boronic acid (17.7 mg, 0.088 mmol) and $\text{Pd}(\text{PPh}_3)_4$ (7.86 mg, 6.80 μmol). The resulting mixture was stirred in microwave under N_2 at 110°C for 20 min. The mixture was then cooled to rt, and solvent was removed *in vacuo*. The residue was purified with silica gel chromatography (eluted with DCM-

MeOH (10:1)) to give 10 mg (35.8%) of the title compound. $^1\text{H-NMR}$ (400 MHz, $\text{MeOH-}d_4$) δ ppm 9.32 (s, 1H), 8.27 (d, $J = 8.5$ Hz, 2H), 8.13 (s, 1H), 8.06 (d, $J = 8.5$ Hz, 2H), 7.49 (d, $J = 1.1$ Hz, 1H), 6.47 – 6.38 (m, 2H), 3.36 (s, 2H), 3.18 (s, 3H). $^{13}\text{C-NMR}$ (101 MHz, $\text{DMSO-}d_6$) δ 155.8, 155.1, 153.4, 152.3, 147.3, 145.6, 143.8, 143.5, 140.3, 132.9, 132.2, 128.7, 128.6, 123.6, 120.8, 120.6, 113.4, 113.2, 107.9, 107.8, 105.7, 71.0, 61.4, 39.7, 36.7, 36.6, 28.0, 24.9, 18. HRMS (ESI): m/z calcd. for $\text{C}_{17}\text{H}_{15}\text{N}_5\text{O}_3\text{S}$ $[\text{M} + \text{H}]^+$ 370.0896, obsd 370.0975.

Xenograft tumor models

All experiments conducted were performed in female athymic balb/c nude mice (Vital River) in an AAALAC certificated facility. All procedures and protocols were approved by the Institutional Animal Care and Use Committee of China Novartis Institute of Biomedical Research. Karpas 422 human B cell lymphoma cells were obtained from the DSMZ cell bank (Germany) and cultured in RPMI-1640 medium (Gibco; 11875-093) supplemented with 15% FBS (Gibco; 10099-141) and 1% Pen Strep (Gibco; 15140-122) at 37°C in an atmosphere of 5% CO_2 in air. Cells were maintained in suspension cultures at concentrations between $0.5 - 2 \times 10^6$ cells/mL. To establish Karpas 422 xenografts cells, were re-suspended in PBS and mixed with Matrigel (BD Bioscience) (1:1, v/v) before injecting 100 μL containing 5×10^6 cells subcutaneously into right flanks of Balb/c nude mice.

In vivo pharmacokinetic/pharmacodynamics and efficacy studies

Compound **43** was used in pharmacokinetic/pharmacodynamics relationship and efficacy studies in animals bearing Karpas 422 xenograft tumors. Tumor volume was determined by measuring the length (L) and perpendicular width (W), with calipers and calculated using the formula: $0.5 \times L \times W^2$. Tumor bearing mice were sorted into treatment groups. Treatment was initiated when the average tumor volume reached 200-400 mm^3 . The compound was formulated as a suspension

in 0.5% PHMC+0.5% Tween 80 in water and administered orally by gavage at a dose volume of 10 mL/kg. At the end point, the animals was given the first dose administration (i.e., the second dose was not given). For PK analysis 100 μ L of blood samples were collected from each animal by orbital sinus bleeding. For analysis of compound levels and PD in tissues, tumors were collected 4 hr post treatment and frozen immediately in liquid nitrogen. When applicable, results are presented as mean \pm SEM. Graphing and statistical analysis was performed using GraphPad Prism 5.00 (GraphPad Software). Tumor and body weight change data were analyzed statistically. If the variances in the data were normally distributed (Bartlett's test for equal variances), the data were analyzed using one-way ANOVA with *post hoc* Dunnett's test for comparison of treatment versus control group. The *post hoc* Tukey test was used for intragroup comparison. Otherwise, the Kruskal-Wallis ranked test *post hoc* Dunn's was used.

As a measure of efficacy the %T/C value is calculated at the end of the experiment according to:

$$(\Delta\text{tumor volume}^{\text{treated}}/\Delta\text{tumor volume}^{\text{control}})*100$$

Tumor regression was calculated according to:

$$-(\Delta\text{tumor volume}^{\text{treated}}/\text{tumor volume}^{\text{treated at start}})*100$$

Where Δ tumor volumes represent the mean tumor volume on the evaluation day minus the mean tumor volume at the start of the experiment.

■ ASSOCIATED CONTENT

Supporting information is available free of charge on ACS Publication website: Synthetic methods for compounds **19** to **23**; characterization data for selected compounds; experimental conditions for crystallization and structure determination; key interactions with EED protein; experimental protocols of biological assays, including alphascreen binding assay, biochemical

and cellular assay; mouse pharmacokinetic study and MTD determination for compound **43**;
molecular formula strings and compound data (CSV)

▪ PDB ACCESSION CODES

Compound **7**: 5H19; compound **8**: 5H24; compound **11**: 5H25. Authors will release the atomic coordinates and experimental data upon article publication.

▪ AUTHOR INFORMATION

Corresponding Author

Phone +86 21 186 2108 2695. E-mail: ying-2.huang@novartis.com

Present Addresses

[§]Novartis Institutes for BioMedical Research, 250 Massachusetts Avenue, Cambridge, Massachusetts 02139, United States

[¶]Novartis Institutes for BioMedical Research, Fabrikstrasse 2, 4056 Basel, Switzerland

[&]Ideaya Biosciences, 280 Utah Avenue, South San Francisco, CA 94080, United States

[¥] Array BioPharma, 3200 Walnut Street, Boulder, CO 80301, United States

[£] Janssen (China) R&D Center, 3F Cheng Kai International Tower, 355 Hong Qiao Road, Shanghai 200030, China

[€]Singapore Centre for Environmental Life Sciences Engineering, 60 Nanyang Drive, SBS-01N-27, Singapore 637551

Notes:

The authors declare no competing financial interest

▪ ACKNOWLEDGMENT

The authors would like to thank Jing Sun, Homan Chan, Chenhui Zeng, Karin Briner, William Sellers and En Li for their support and insightful discussions.

▪ ABBREVIATIONS USED

PRC, Polycomb repressive complex; EED, Embryonic ectoderm development; H3K27, histone H3 lysine 27; SAM, S-adenosylmethionine; HTRF, homogeneous time resolved fluorescence; SAH, S-adenosyl-l-homocysteine hydrolase; HTS, high-throughput screen; NMR, nuclear magnetic resonance; DMSO, dimethyl sulfoxide; HAC, heavy atom count; LE, ligand efficiency; LipE, lipophilic efficiency; SAR, structure-activity relationship; HPLC, High Performance Liquid Chromatography.

▪ REFERENCES

-
- (1) (a) Liu, F.; Wang, L.; Perna, F.; Nimer, S. D. Beyond transcription factors: how oncogenic signaling reshapes the epigenetic landscape. *Nat. Rev. Cancer* **2016**, *16*, 359-372. (b) Jones, P. A.; Baylin, S. B. The fundamental role of epigenetic event in cancer. *Nat. Rev. Genet.* **2002**, *3*, 419-428.
- (2) (a) Greer, E. L.; Shi, Y. Histone methylation: a dynamic mark in health, disease and inheritance. *Nat. Rev. Genet.* **2012**, *13*, 343-357. (b) Copeland, R. A.; Solomon, M. E.; Richon, V. M. Protein methyltransferases as a target class for drug discovery. *Nat. Rev. Drug Discovery* **2009**, *8*, 725-732. (c) Zagni C.; Chiacchio U; Rescifina A. Histone methyltransferase inhibitors: novel epigenetic agents for cancer treatment. *Curr. Med. Chem.* **2013**, *20*, 167-185.
- (3) (a) Margueron, R.; Reinberg, D. The Polycomb complex PRC2 and its mark in life. *Nature* **2011**, *469*, 343-349. (b) Xu, C.; Bian, C.; Yang, W.; Galka, M.; Ouyang, H.; Chen, C.; Qiu, W.; Liu, H.; Jones, A. E.; MacKenzie, F.; Pan, P.; Li, S.-C.; Wang, H.; Min, J. Binding of different histone marks differentially regulates the activity and specificity of Polycomb Repressive Complex 2 (PRC2). *Proc. Natl. Acad. Sci.* **2010**, *107*, 19266-19271.

- (4) (a) Kim, K. H.; Roberts, C. W. M. Targeting EZH2 in Cancer. *Nat. Med.* **2016**, *22*, 128–134.
- (b) Xu, B.; Konze, K. D.; Jin, J.; Wang, G. G. Targeting EZH2 and PRC2 dependence as novel anticancer therapy. *Exp. Hematol.* **2015**, *43*, 698–712. (c) McCabe, M. T.; Creasy, C. L. EZH2 as a potential target in cancer therapy. *Epigenomics* **2014**, *6*, 341–351. (d) Varambally, S.; Dhanasekaran, S. M.; Zhou, M.; Barrette, T. R.; Kumar-Sinha, C.; Sanda, M. G.; Ghosh, D.; Pienta, K. J.; Sewalt, R. G. A. B.; Otte, A. P.; Rubin, M. A.; Chinnaiyan, A. M. The Polycomb group protein EZH2 is involved in progression of prostate cancer. *Nature* **2002**, *419*, 624–629.
- (e) Morin, R. D.; Johnson, N. A.; Severson, T. M.; Mungall, A. J.; An, J.; Goya, R.; Paul, J. E.; Boyle, M.; Woolcock, B. W.; Kuchenbauer, F.; Yap, D.; Humphries, R. K.; Griffith, O. L.; Shah, S.; Zhu, H.; Kimbara, M.; Shashkin, P.; Charlot, J. F.; Tcherpakov, M.; Corbett, R.; Tam, A.; Varhol, R.; Smailus, D.; Moksa, M.; Zhao, Y.; Delaney, A.; Qian, H.; Birol, I.; Schein, J.; Moore, R.; Holt, R.; Horsman, D. E.; Connors, J. M.; Jones, S.; Aparicio, S.; Hirst, M.; Gascoyne, R. D.; Marra, M. A. Somatic mutations altering EZH2 (Tyr641) in follicular and diffuse large B-Cell lymphomas of germinal-center origin. *Nat. Genet.* **2010**, *42*, 181–185. (f) Takawa, M.; Masuda, K.; Kunizaki, M.; Daigo, Y.; Takagi, K.; Iwai, Y.; Cho, H.-S.; Toyokawa, G.; Yamane, Y.; Maejima, K.; Field, H. I.; Kobayashi, T.; Akasu, T.; Sugiyama, M.; Tsuchiya, E.; Atomi, Y.; Ponder, B. A. J.; Nakamura, Y.; Hamamoto, R. Validation of the histone methyltransferase EZH2 as a therapeutic target for various types of human cancer and as a prognostic marker. *Cancer Sci.* **2011**, *102*, 1298–1305. (g) Kemp, C. D.; Rao, M.; Xi, S.; Inchauste, S.; Mani, H.; Fetsch, P.; Filie, A.; Zhang, M.; Hong, J. A.; Walker, R.; L.; Zhu, Y. J.; Ripley, R. T.; Mathur, A.; Liu, F.; Yang, M.; Meltzer, P. A.; Marquez, V. E.; De Rienzo, A.; Bueno, R.; Schump, D. S. Polycomb repressor complex-2 is a novel target for mesothelioma therapy. *Clin. Cancer. Res.* **2012**, *18*, 77–90.

- (5) (a) Montgomery, N. D.; Yee, D.; Chen, A.; Kalantry, S.; Chamberlain, S. M. The murine Polycomb group protein EED is required for global histone H3 Lysine-27 methylation genetic or RNAi-based approaches of PRC2 core. *Curr. Bio.* **2005**, *15*, 942–947. (b) Pasini, D.; Bracken, A. P.; Jensen, M. R.; Denchi E. L.; Helin, K. Suz12 is essential for mouse development and for EZH2 histone methyltransferase activity. *EMBO J.* **2004**, *23*, 4061–4071.
- (6) (a) Margueron, R.; Justin, N.; Ohno, K.; Sharpe, M. L.; Son, J.; Drury, W. J.; Voigt, P.; Martin, S. R.; Taylor, W. R.; De Marco, V.; Pirrotta, V.; Reinberg, D.; Gambin, S. J. Role of the Polycomb Protein EED in the propagation of repressive histone marks. *Nature* **2009**, *461*, 762–767. (b) Cao, Q.; Wang, X.; Zhao, M.; Yang R.; Rohit, M. R.; Qiao, Y.; Anton, P. A.; Anastasia K; Yocum, A. K.; Li, Y.; Chen W.; Cao, X.; Jiang, X.; Dahiya, A.; Harris, C.; Feng, F. Y.; Kalantry, S.; Qin, Z. S.; Dhanasekaran, S. M.; Chinnaiyan, A. M. The central role of EED in the orchestration of polycomb group complexes. *Nat. Commun.* **2014**, *5*, 3127-3140.
- (7) (a) Margueron, R.; Li, G.; Sarma, K. EZH1 and EZH2 maintain repressive chromatin through different mechanisms. *Molecular Cell* **2008**, *32*, 503-518. (b) Shen, X.; Liu, Y.; Hsu, Y.-J. EZH1 mediates methylation on histone H3 lysine 27 and complements EZH2 in maintaining stem cell identity and executing pluripotency. *Molecular Cell* **2008**, *32*, 491-502.
- (8) Hayden, A.; Johnson, P.W.; Packham, G.; Crabb, S. J. S-Adenosylhomocysteine hydrolase inhibition by 3-deazaneplanocin A analogues induces anti-cancer effects in breast cancer cell lines and synergy with both histone deacetylase and HER2 inhibition. *Breast Cancer Res. Treat.* **2010**, *127*, 109-119.
- (9) Knutson, S. K.; Wigle, T. J.; Warholc, N. M.; Sneeringer, C. J.; Allain, C. J.; Klaus, C. R.; Sacks, J. D.; Raimondi, A.; Majer, C. R.; Song, J.; Scott, M. P.; Jin, L.; Smith, J. J.; Olhava, E. O.; Chesworth, R.; Moyer, M. P.; Richon, V. M.; Copeland, R. A.; Keilhack, H.; Pollock, R. M.;

Kuntz, K. W. A selective inhibitor of EZH2 blocks H3K27 methylation and kills mutant lymphoma cells. *Nat. Chem. Biol.* **2012**, *8*, 890–896.

(10) McCabe, M. T.; Ott, H. M.; Ganji, G.; Korenchuk, S.; Thompson, C.; Van Aller, G. S.; Liu, Y.; Graves, A. P.; Pietra III, A. D.; Diaz, E.; LaFrance, L. V.; Mellinger, M.; Duquenne, C.; Tian, X.; Kruger, R. G.; McHugh, C. F.; Brandt, M.; Miller, W. H.; Dhanak, D.; Verma, S. K.; Tummino, P. J.; Creasy, L. C. EZH2 inhibition as a therapeutic strategy for lymphoma with EZH2-activating mutations. *Nature* **2012**, *492*, 108–112.

(11) Konze, K.D.; Ma, A.; Li, F.; Barsyte-Lovejoy, D. B.; Parton, T.; MacNevin, C. J.; Liu, F.; Gao, C.; Huang, X.-P.; Kuznetsova, E.; Rougie, M.; Jiang, A.; Pattenden, S. G.; Jacqueline L. Norris, J. L.; James, L. I.; Roth, B. L.; Brown, P. L.; Frye, S. V.; Arrowsmith, C. H.; Hahn, K. M.; Wang, G. G.; Vedadi, M.; Jin, J. An orally bioavailable chemical probe of the lysine methyltransferases EZH2 and EZH1 *ACS Chem. Biol.* **2013**, *8*, 1324–1334.

(12) (a) Knutson, S. K.; Warholic, N. M.; Wigle T. J.; Klaus, C. R.; Allain, C. J.; Raimondi, A.; Scott, P. M.; Chesworth, R.; Moyer, M. P.; Copeland, R. A.; Richon, V. M.; Pollock, R. M.; Kuntz, K. W.; Keilhack, H. Durable tumor regression in genetically altered malignant rhabdoid tumors by inhibition of methyltransferase EZH2. *Proc. Natl. Acad. Sci.* **2013**, *110*, 7922–7927.

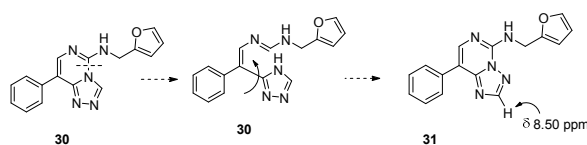
(b) Knutson, S. K.; Kawano, S.; Minoshima, Y.; Warholic, N. M.; Huang, K.-C.; Xiao Y.; Kadowaki, T.; Uesugi, M.; Kuznetsov, G.; Kumar, N.; Wigle, T. J.; Klaus, C. R.; Allain, C. J.; Raimondi, A.; Waters, N. J.; Smith, J. J.; Porter-Scott, M.; Chesworth, R.; Moyer, M. P.; Copeland, R. A.; Richon, V. M.; Uenaka, T.; Pollock, R. M.; Kuntz, K. W.; Yokoi, A.; Keilhack, H. Selective inhibition of EZH2 by EPZ-6438 leads to potent antitumor activity in EZH2-mutant non-Hodgkin lymphoma. *Mol. Cancer Ther.* **2014**, *13*, 842–854.

- (13) Vaswani, R. G.; Gehling, V. S.; Dakin, L. A.; Cook, A. S.; Christopher G.; Nasveschuk, C. G.; Duplessis, M.; Iyer, P.; Balasubramanian, S.; Zhao, F.; Good, A. C.; Campbell, R.; Lee, C.; Cantone, N.; Cummings, R. T.; Normant, E.; Bellon, S. F. Albrecht, B. K. Harmange, J.-C.; Trojer, P.; Audia, J. E. Zhang, Y.; Justin, N.; Chen, S.; Wilson, J. R.; Gamblin, S. J. Identification of (R)-N-((4-methoxy-6-methyl-2-oxo-1,2-dihydropyridin-3-yl)methyl)-2-methyl-1-(1-(1-(2,2,2-trifluoroethyl)piperidin-4-yl)ethyl)-1H-indole-3-carboxamide (CPI-1205), a potent and selective inhibitor of histone methyltransferase EZH2, suitable for Phase I clinical trials for B-Cell lymphomas. *J. Med. Chem.* **2016**, 59, 9928–9941.
- (14) (a) Jiao, L.; Liu, X. Structural basis of histone H3K27 trimethylation by an active polycomb repressive complex 2. *Science*, **2015**, DOI:10.1126/science.aac4383. (b) Justin, N.; Zhang, Y.; Tarricone, C.; Stephen R.; Martin, S. R.; Chen, S.; Underwood, E.; De Marco, V.; Haire, L. F.; Walker, P. A.; Reinberg, D.; Wilson, J. R.; Gamblin, S. J. Structural basis of oncogenic histone H3K27M inhibition of human polycomb repressive complex 2. *Nat. Commun.* **2016**, doi:10.1038/ncomms11316.
- (15) For details of our hit finding effort including confirmed hits and their X-crystal structures: Li, L.; Zhang, H.; Zhang, M.; Zhao, M.; Feng, L.; Luo, X.; Gao, Z.; Huang, Y.; Ardayfio, O.; Zhang, J. Lin, Y.; Fan, H.; Mi, Y.; Li, G.; Liu, L.; Feng, G.; Luo, F.; Teng, L.; Qi, W.; Ottl, J.; Lingel, A.; Bussiere, D. E.; Yu, Z.; Atadja, P.; Lu, C.; Li, E.; Gu, J.; Zhao, K. Novel inhibitors of polycomb repressive complex 2 through allosteric EED binding. *PLoS One* **2017**, 12 (1), e016985
- (16) Santiago, C.; Nguyen, K.; Schapira, M. Druggability of methyl-lysine binding sites. *J. Comput.-Aided Mol. Des.* **2011**, 25, 1171–1178.

(17) Li, S.; Gu, X. J.; Hao, Q.; Fan, H.; Li, L.; Zhou, S.; Zhao, K.; Chan, H. M.; Wang, Y. K. A liquid chromatography/mass spectrometry-based generic detection method for biochemical assay and hit discovery of histone methyltransferases. *Anal. Biochem.* **2013**, *443*, 214-221.

(18) To understand how the binding to EED affects the EZH2 methylation activity, we have studied the mechanism of action of our EED compounds. Using compound **43** as an example, we established evidences that our compounds bind directly to the K27Me3 pocket.: Qi, W.; Zhao, K.; Gu, J.; Huang, Y.; Wang, Y.; Zhang, H.; Zhang, M.; Zhang, J.; Yu, Z.; Li, L.; Teng, L.; Chuai, S.; Zhang, C.; Zhao, M.; Chan, H.; Chen, Z.; Fang, D.; Fei, Q.; Leying Feng, L.; Feng, L.; Gao, Y.; Ge, H.; Ge, X.; Li, G.; Lingel, A.; Lin, Y.; Liu, Y.; Luo, F.; Shi, M.; Wang, L.; Wang, Z.; Yu, Y.; Zeng, J.; Zeng, C.; Zhang, L.; Zhang, Q.; Zhou, S.; Oyang, C.; Atadja, P.; Li, E. Unpublished results.

(19) Brown, D. J.; Nagamatsu, T. Isomerizations akin to the Dimroth rearrangement III the conversion of simple s-triazols [4,3-a] pyrimidines into their [1,5-a] isomers. *Aust. J. Chem.* **1977**, *30*, 2515-2525.



(20) For excellent review on liability of furan: Peterson, L. A. Reactive metabolites in the biotransformation of molecules containing a furan ring. *Chem. Res. Toxicol.* **2013**, *26*, 6–25.

(21) Bowes J.; Brown, A. J.; Hamon J.; Jarolimek, W.; Sridhar A.; Waldron, G.; Whitebread, S. Reducing safety-related drug attrition: the use of in vitro pharmacological profiling. *Nat. Rev. Drug Discovery* **2012**, *11*, 909-922.

Table of Content Graphic

